Science Advances
AAAS

advances.sciencemag.org/cgi/content/full/5/8/eaax4111/DC1

Supplementary Materials for

Weakening Atlantic Niño–Pacific connection under greenhouse warming

Fan Jia, Wenju Cai*, Lixin Wu*, Bolan Gan, Guojian Wang, Fred Kucharski, Ping Chang, Noel Keenlyside

*Corresponding author. Email: wenju.cai@csiro.au (W.C.); lxwu@ouc.edu.cn (L.W.)

Published 21 August 2019, *Sci. Adv.* **5**, eaax4111 (2019)
DOI: 10.1126/sciadv.aax4111

This PDF file includes:

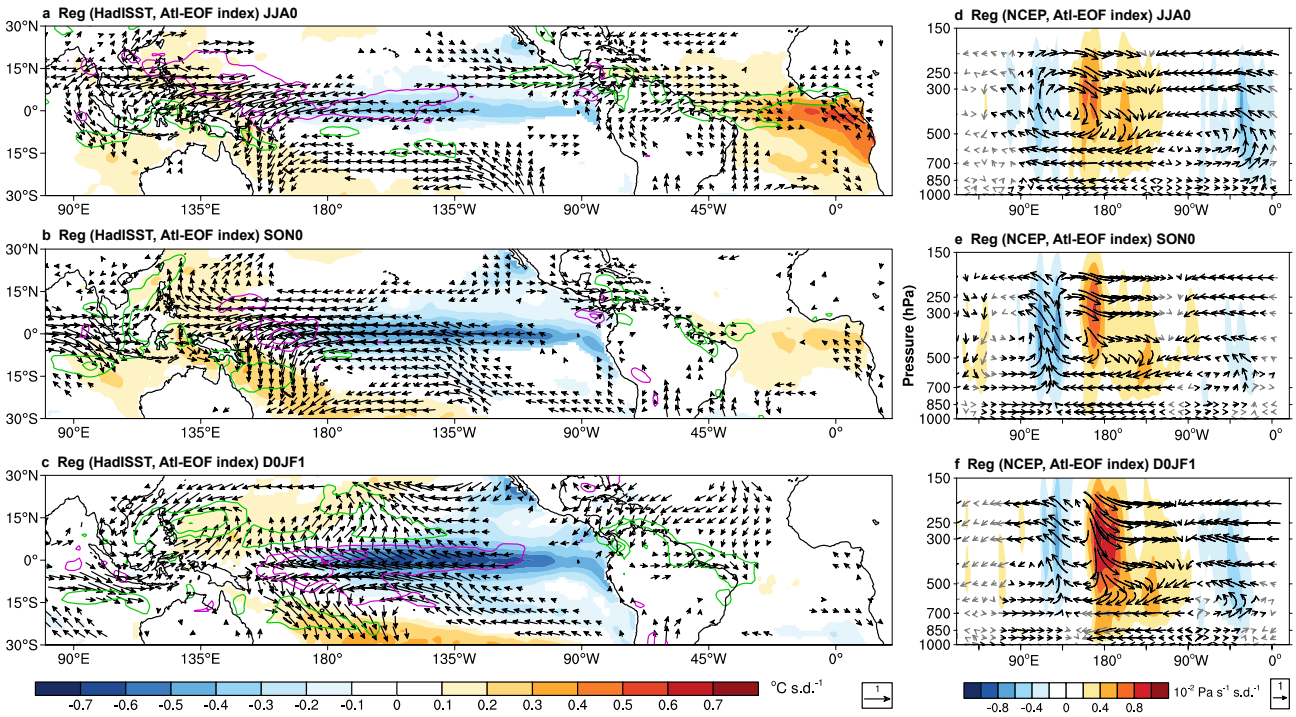

Fig. S1. Observed development of the Atlantic Niño–Pacific connection. Lagged regressions of observed seasonal SST (ºC; shaded in the left column), wind vector at 925 hPa (m s^{-1}; vectors in the left column), precipitation (purple and green contours in the left column indicate negative and positive precipitation anomalies respectively; the minimum contour is ± 0.5 mm day^{-1} with ± 0.5 mm day^{-1} intervals), vertical equatorial (10ºS-10ºN) atmospheric velocity (Pa s^{-1}; shaded in the right column) and equatorial atmospheric vector (zonal wind and vertical velocity scaled by a factor of 300; vectors in the right column) during JJA0 (**a**, **d**), SON0 (**b**, **e**) and D0JF1 (**c**, **f**) seasons onto the Atl-EOF index. Only the values at the 95% confidence level or higher are shown except for the vector sections in the right column, where gray vectors indicate values not significant. The color maps and reference vectors for the left (a-c) and right (d-f) columns are labeled in the bottom left and right, respectively.

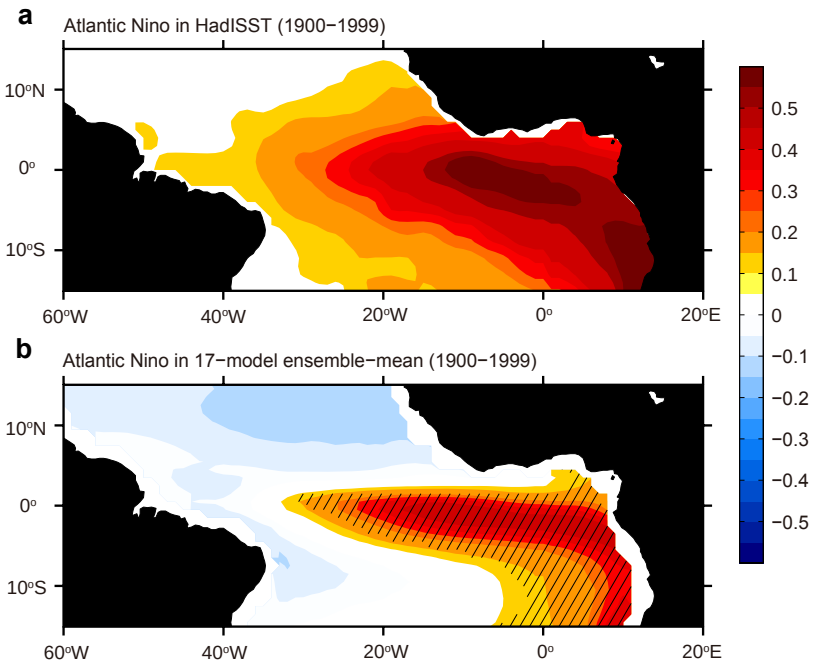

Fig. S2. Comparison of Atlantic Niño patterns in observation and 17 selected models. Atlantic Niño pattern over the 1900-1999 period by regressing the SST anomalies onto the Atl-EOF index derived from HadISST (**a**) and multi-model ensemble-mean of the 17 selected models (**b**). The most robust features of ensemble where the mean exceeds one standard deviation in **b** are hatched.

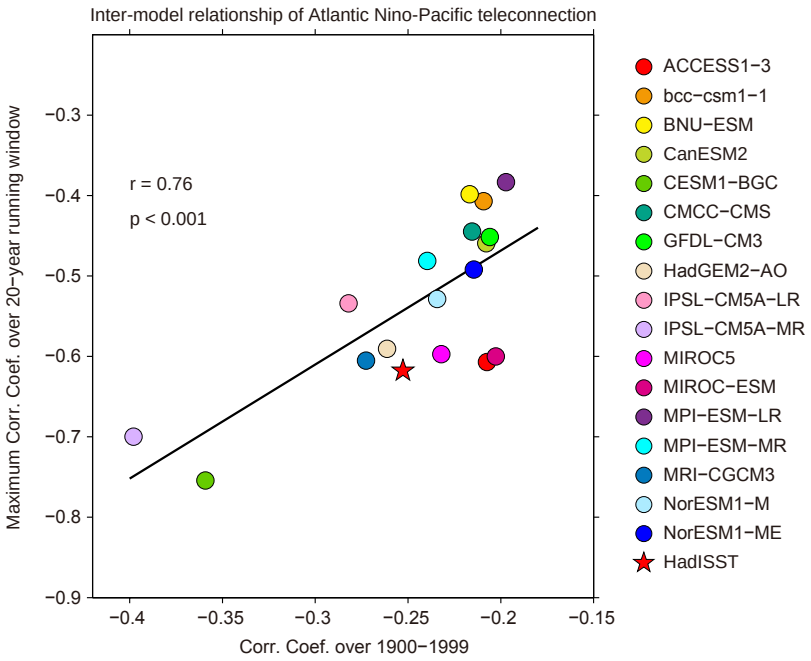

Fig. S3. Intermodel relationship of Atlantic Niño–Pacific teleconnection over 100 years and its multidecadal fluctuations. X-axis: Sign-dependent average correlation coefficients (see Materials and Methods section 'Sign-dependent average correlations') of the Atl-EOF index (JJA0) and the grid-point D0JF1 equatorial Pacific (5º S-5º N, 160º E-90º W) SST anomalies over the 1900-1999 period. Y-axis: Maximum correlation in the evolution of correlations obtained using 20-year sliding windows over the same 100-year period. The linear fits (solid lines) is displayed together with the correlation coefficient r and P value from the regression.

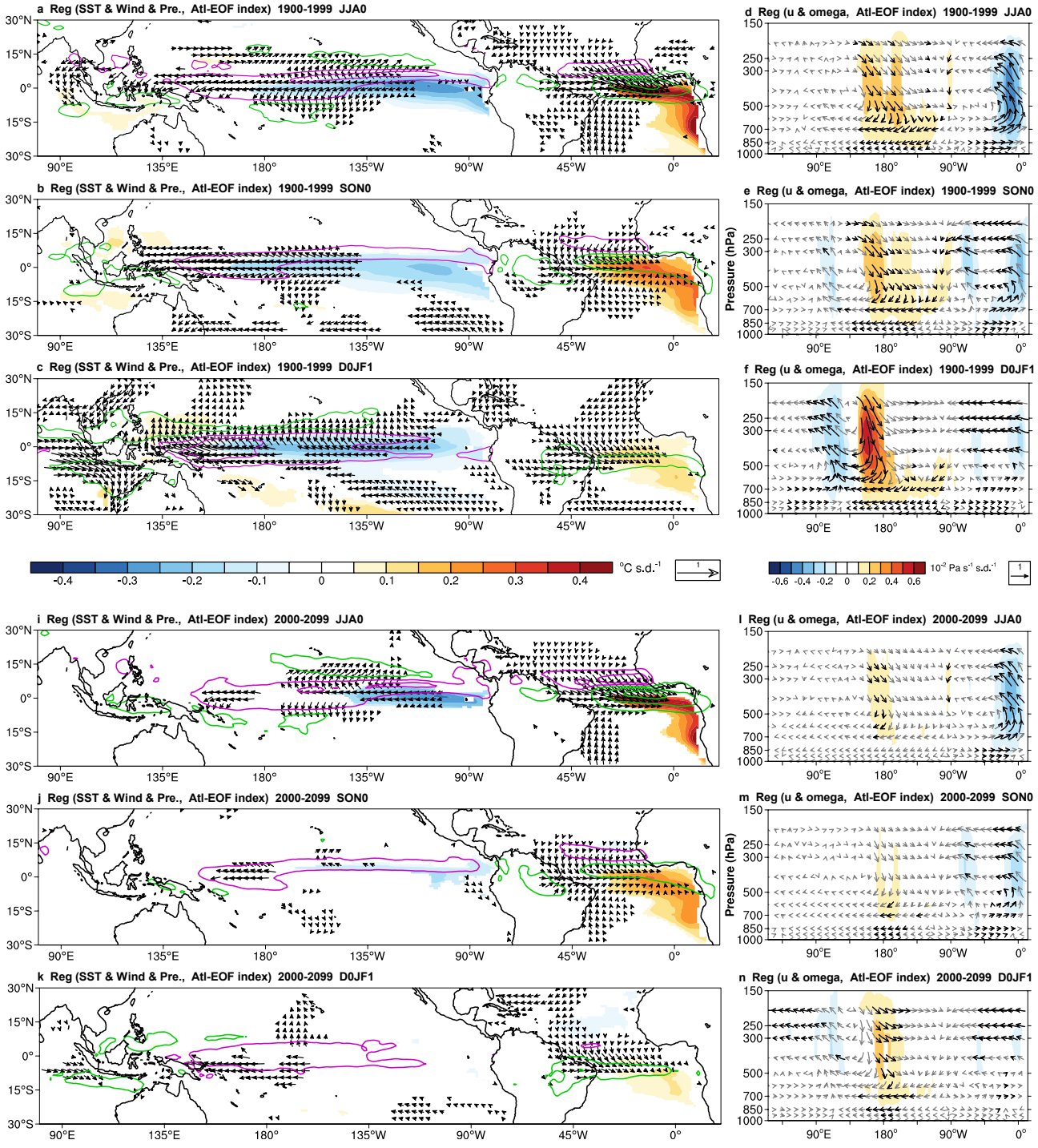

Fig. S4. Modeled development of the Atlantic Niño–Pacific teleconnection. Same as those in fig. S1 but for the multi-model ensembled regressions of the 17 selected models under present-day climate (1900-1999) (**upper, a-f**) and future climate (2000-2099) (**lower, i-n**). The minimum contour is ± 0.2 mm day^{-1} with ± 0.4 mm day^{-1} intervals for the precipitation.

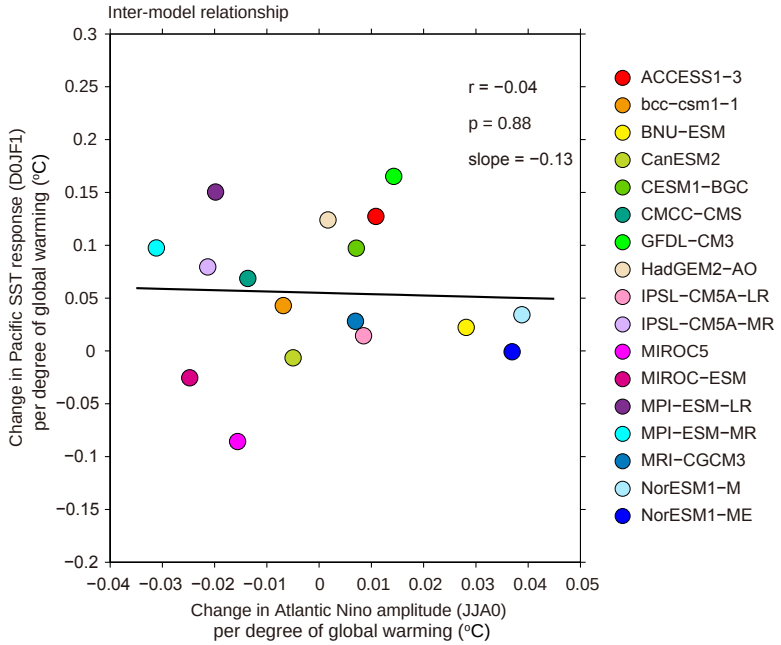

Fig. S5. Impact of the Atlantic Niño amplitude change on the Pacific SST response. Inter-model relationship between changes in the amplitude of Atlantic Niño (x axis) and Pacific SST response (y axis). The linear fitting line (black solid line) and correlation coefficients are also shown. The amplitude of Atlantic Niño is obtained by averaging the regressed SST (onto the Atl-EOF index) in the equatorial Atlantic (5° S-5° N, 45° W-20° E) during JJA0. The Pacific SST response is measured by the sign-dependent average regression coefficients (see Materials and Methods section 'Sign-dependent average correlations') of the grid-point D0JF1 equatorial Pacific (5° S-5° N, 160° E-90° W) SST anomalies onto the Atl-EOF index. To enhance the inter-model comparability, the changes are scaled by the increase in global-mean temperature over the present-day and future periods. The linear fits (solid lines) is displayed together with the correlation coefficient r, slope and P value from the regression.

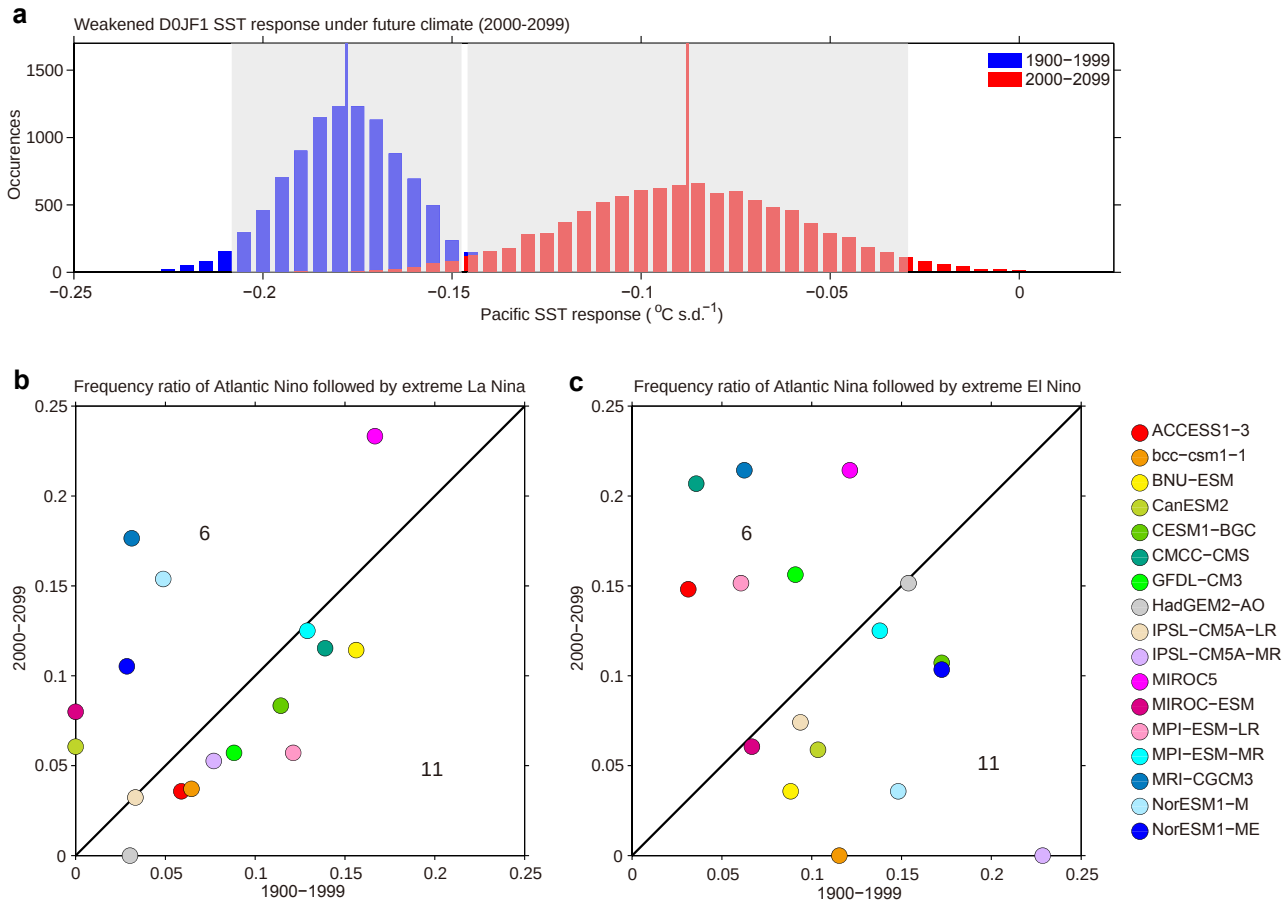

Fig. S6. Projected decrease in the Atlantic Niño–Pacific connection in terms of bootstrap test and extreme ENSO. a, Histograms of 10,000 realizations of a bootstrap method for the Pacific SST response. The Pacific SST response is measured by the sign-dependent average regression coefficients (see Materials and Methods section 'Sign-dependent average correlations') of the grid-point D0JF1 equatorial Pacific (5º S-5º N, 160º E-90º W) SST anomalies onto the Atl-EOF index. The blue and red vertical lines indicate the mean values of 10,000 inter-realizations for the present-day and future periods, respectively. The grey shaded regions indicate the respective two standard deviations (the 95% confidence interval based on normal distribution) of the 10,000 inter-realization (see Materials and Methods section 'Bootstrap test'). (**b**, **c**) Comparison of the occurrence ratio of Atlantic Niño (Atl-EOF index > 0.5 s.d.) followed by extreme La Niña (C-index < -1.75 s.d.) over the total Atlantic Niño events (a) and that of Atlantic Niña (Atl-EOF index < -0.5 s.d.) followed by extreme El Niño (E-index > 1.5 s.d.) over the total Atlantic Niña events over the present-day (1900-1999; blue bars) and future (2000-2099; red bars) 100-year periods in the 17 selected models (see Materials and Methods section 'E-index and C-index'). Numbers in the upper left (lower right) indicate the number of models that produce stronger (weaker) impact of Atlantic Niño/Niña on extreme ENSO under future climate.

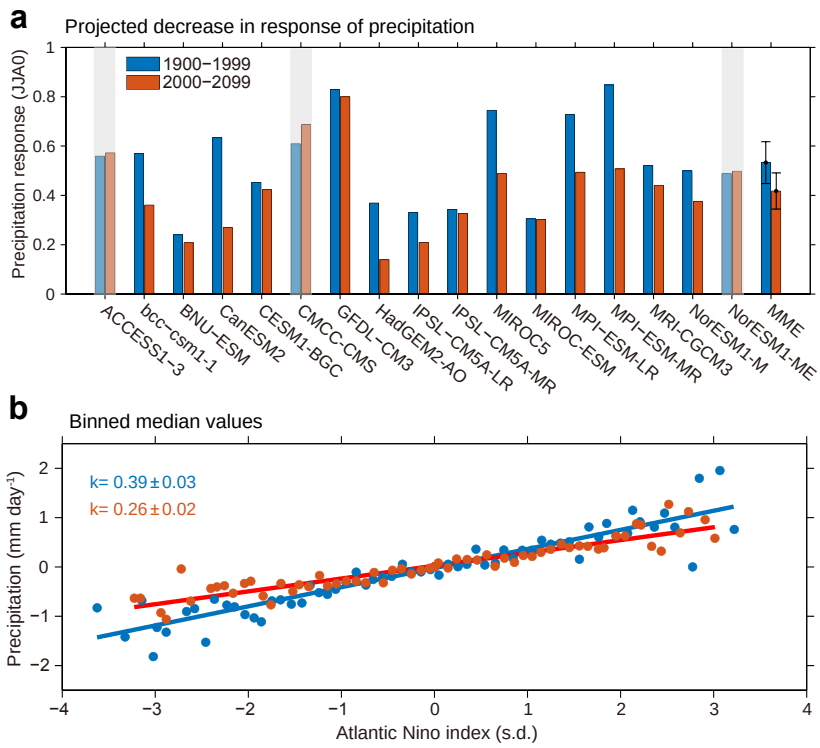

Fig. S7. Projection of decreased precipitation response to a diabatic equatorial Atlantic heating. **a**, Comparison of precipitation response to the Atl-EOF index over the present-day (blue bars) and future (red bars) 100-year periods in the 17 selected models. The three models that simulate an increase in response are marked in grey. Error bars in the multi-model mean are calculated as two standard deviations (the 95% confidence interval based on normal distribution) of the 10,000 inter-realizations of a bootstrap method (see Materials and Methods section 'Bootstrap test'). The precipitation response is measured by the regression coefficients (mm day^{-1} s.d. $^{-1}$) of the JJA0 precipitation anomalies averaged over the equatorial Atlantic (5^{o} S-5^{o} N, 45^{o} W-20^{o} E) and the respective Atl-EOF index. **b**, Response of JJA0 precipitation anomalies averaged over the equatorial Atlantic (5^{o} S-5^{o} N, 45^{o} W-20^{o} E) (mm day^{-1}) to JJA0 Atl-EOF index using all samples of 17 selected models. The precipitation anomalies are binned in 0.1-s.d. Atl-EOF index intervals, and the median precipitation anomaly and index are identified for each bin (dots). Blue and red dots indicate values in the present-day and future 100-year periods, respectively. The corresponding linear fitting lines (with the values of the slopes plus and minus the 95% confidence values from the Student's *t*-test) are also shown.

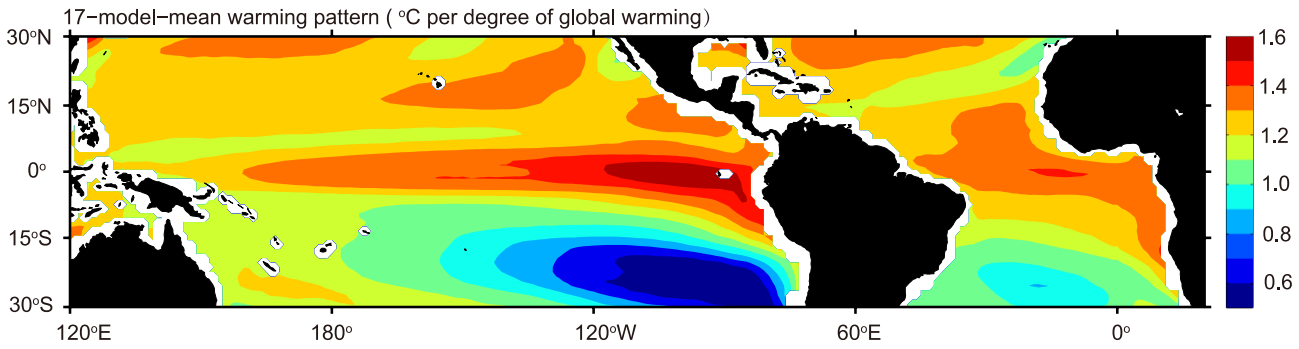

Fig. S8. Projected warming pattern of equatorial Pacific and Atlantic Ocean. Multi-model ensemble-mean change in tropical SST between future (2000-2099) and present-day (1900-1999) climates. To enhance the inter-model comparability, the changes are scaled by the increase in global-mean temperature over the present-day and future periods.

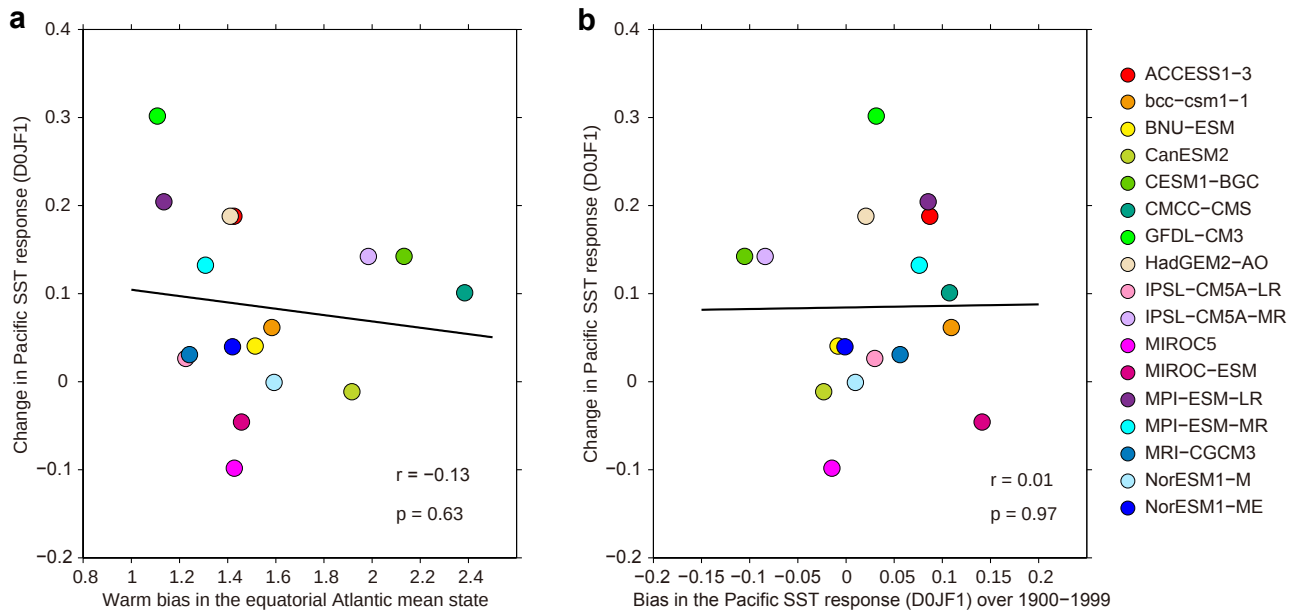

Fig. S9. Impact of model biases on the Pacific SST response. Inter-model relationship of bias in the equatorial Atlantic mean state (**a**, x axis) and bias in the Atlantic Niño-Pacific connection (**b**, x axis) over the present-day climate (1900-1999) with changes in the boreal-winter Pacific SST response (y axis). The Pacific SST response is measured by the sign-dependent average regression coefficients (see Materials and Methods section 'Sign-dependent average correlations') of the grid-point D0JF1 equatorial Pacific (5° S-5° N, 160° E-90° W) SST anomalies onto the Atl-EOF index. The bias in the equatorial Atlantic mean state is measured by the difference of climatological mean SST over the equatorial Atlantic (5° S-5° N, 45° W-20° E) during 1900-1999 between models and observation. The bias in the Atlantic Niño-Pacific connection is measured by the difference of boreal-winter Pacific SST response during 1900-1999 between models and observation. The linear fits (solid lines) is displayed together with the correlation coefficient r and P value from the regression.

Table S1. Observed relationship between ENSO events and the Atlantic Niño. The El Niño (La Niña) events are defined based on NOAA's criterion that the ONI [3 month running mean of ERSST.v5 SST anomalies in the Niño 3.4 region (5ºN-5ºS, 120º-170ºW)] be greater (less) than or equal to +0.5 °C (-0.5 °C) for a period of at least five consecutive overlapping 3-month seasons. The Atlantic Niño (Atlantic Niña) events are defined by the Atl-EOF index (i.e., normalized PC1 of quadratically detrended SST anomalies averaged in JJA0) be greater (less) than or equal to +0.5 s.d. (-0.5 s.d.). In total, there are 10 out of 17 Atlantic Niño events that are followed by La Niña (labeled in red), and 8 out of 17 Atlantic Niña events followed by El Niño events (labeled in blue) from 1965 to 2017.

Year	Atlantic Niño/Niña	ENSO
1965	Atlantic Niña	El Niño
1966	Atlantic Niño	Neutral
1967	Atlantic Niña	Neutral
1968	Atlantic Niño	El Niño
1969	Atlantic Niña	El Niño
1970	Atlantic Niña	La Niña
1973	Atlantic Niño	La Niña
1974	Atlantic Niño	La Niña
1976	Atlantic Niña	El Niño
1977	Atlantic Niña	El Niño
1978	Atlantic Niña	Neutral
1980	Atlantic Niña	Neutral
1982	Atlantic Niña	El Niño
1983	Atlantic Niña	La Niña
1984	Atlantic Niño	La Niña
1987	Atlantic Niño	El Niño
1988	Atlantic Niño	La Niña
1989	Atlantic Niño	Neutral

Year	Atlantic Niño/Niña	ENSO
1990	Atlantic Niña	Neutral
1992	Atlantic Niña	Neutral
1994	Atlantic Niña	El Niño
1995	Atlantic Niño	La Niña
1996	Atlantic Niño	Neutral
1997	Atlantic Niña	El Niño
1998	Atlantic Niño	La Niña
1999	Atlantic Niño	La Niña
2005	Atlantic Niña	La Niña
2006	Atlantic Niño	El Niño
2008	Atlantic Niño	La Niña
2010	Atlantic Niño	La Niña
2012	Atlantic Niña	Neutral
2015	Atlantic Niña	El Niño
2016	Atlantic Niño	Neutral
2017	Atlantic Niño	La Niña
Total	Atlantic Niño (17)	Followed by La Niña (10)
	Atlantic Niña (17)	Followed by El Niño (8)

Table S2. CMIP5 models and their EOF modes of tropical Atlantic used in this study. Names of models, the associated institutions and countries, and the EOF mode of tropical Atlantic selected to represent the Atlantic Niño as well as Atlantic Niño-Pacific teleconnection.

Model name	Institute	Country	EOF mode
1. ACCESS1-0	Commonwealth Scientific and Industrial Research Organization/Bureau of Meteorology	Australia	1
2. ACCESS1-3			1
3. bcc-csm1-1	Beijing Climate Center, China Meteorological Administration	China	1
4. bcc-csm1-1-m			1
5. BNU-ESM	Beijing Normal University	China	2
6. CanESM2	Canadian Centre for Climate Modelling and Analysis	Canada	1
7. CCSM4	National Center for Atmospheric Research	United States	1
8. CESM1-BGC			1
9. CESM1-CAM5			1
10. CMCC-CESM	Centro Euro-Mediterraneo per I Cambiamenti Climatici	Germany	1
11. CMCC-CM			1
12. CMCC-CMS			2
13. CNRM-CM5	Météo-France/Centre National de Recherches Météorologiques	France	1
14. CSIRO-MK-3.6.0	Commonwealth Scientific and Industrial Research Organisation in collaboration with the Queensland Climate Change Centre of Excellence	Australia	1
15. FGOALS-g2	The First Institute of Oceanography, SOA	China	1
16. GFDL-CM3	National Oceanic and Atmospheric Administration/Geophysical Fluid Dynamics Laboratory	United States	1
17. GFDL-ESM2G			1
18. GFDL-ESM2M			1
19. GISS-E2-H	National Aeronautics and Space Administration/Goddard Institute for Space Studies	United States	1
20. GISS-E2-R			1
21. HadGEM2-A0	Met Office Hadley Centre	United Kingdom	2
22. HadGEM2-ES			1
23. INM-CM4	Institute for Numerical Mathematics	Russia	1
24. IPSL-CM5A-MR	Institute Pierre Simon Laplace	France	2
25. IPSL-CM5A-LR			2
26. IPSL-CM5B-LR			2
27. MIROC5	University of Tokyo, Atmosphere and Ocean Research Institute; National Institute for Environmental Studies; Japan Agency for Marine Earth Science and Technology	Japan	1
28. MIROC-ESM			1
29. MPI-ESM-LR	Max Planck Institute for Meteorology	Germany	2
30. MPI-ESM-MR			2
31. MRI-CGCM3	Meteorological Research Institute	Japan	2
32. NorESM1-M	Norwegian Climate Centre	Norway	1
33. NorESM1-ME			1